Advances in Materials
2013; 2(1) : 1-5
Published online February 20, 2013 (http://www.sciencepublishinggroup.com/j/am)
doi: 10.11648/j.am.20130201.11

Corrosion behaviour of CNT reinforced AA 7075 nanocomposites

B. Thirumaran[1], S. Natarajan[1,2,*], S. P. Kumaresh[1,2]

[1]Department of Metallurgical and Materials Engineering, National Institute of Technology, Tiruchirappalli
[2]Centre of Excellence in Corrosion and Surface Engineering, National Institute of Technology, Tiruchirappalli

Email address:
truemaran@yahoo.co.in (B. Thirumaran), cecase@nitt.edu, sn@nitt.edu, (S. Natarajan), babu@nitt.edu (S.P.Kumaresh Babu)

To cite this article:
B. Thirumaran, S. Natarajan, S. P. Kumaresh. Corrosion Behaviour of CNT Reinforced AA 7075 Nanocomposites. *Advances in Materials*. Vol. 2, No. 1, 2013, pp. 1-5. doi: 10.11648/j.am.20130201.11

Abstract: Carbon nanotubes reinforced AA 7075 alloy was fabricated by powder metallurgy route. Multi-walled carbon nanotubes (MWCNTs) were synthesized by electric arc discharge method. Different mass fraction of CNTs was added to the AA 7075 and the powder mixtures were consolidated using uniaxial press. The consolidated samples were sintered at 600˚ C in inert atmosphere followed by hot compaction at 450˚ C. The electrochemical corrosion behaviour of AA 7075 and CNT reinforced AA 7075 was studied using Electrochemical Polarization Technique (ACM Gill) and Electrochemical Impedance Technique. The relative densities of the composites were measured. The phase analysis and surface morphology of the composites were done by XRD and scanning electron microscope (SEM). The corrosion behaviour of the composites and the possible mechanism for the effect of CNT in the properties have been studied in detail in this paper.

Keywords: AA 7075, Composite, CNT, Arc Discharge, Sintering, Electrochemical Corrosion, Impedance Spectroscopy, XRD, Raman Spectroscopy, SEM & TEM

1. Introduction

CNT can be thought of as one or more graphite sheets which have been wrapped up into a seamless cylinder. Since their discovery in 1991 by Iijima [1], the path breaking mechanical property of these structures has received much attention. The high strength and other high mechanical properties of MWNT and SWNT have been probed expe-rimentally, and show a good correspondence with the theo-retical prediction. In this paper, the fabrication of the Al-CNT composites, the investigation of the microstructure and the measurement of the corrosion resistance of the composites are reported. Among various useful aluminium alloys, AA 7075 alloy is characterized by rea-sonable corrosion resistance and high strength. Further, this alloy is often used as the base metal for metal matrix composites (MMCs) reinforced by various non-metallic fibres, particles and whiskers. The corrosion resistance of a metal tends to be adversely affected by the presence of a second phase. The only exception may be ferritic-austenitic stainless steel. The literature [2–10] on the corrosion beha-viour of MMCs has shown that the presence of a reinforcing material may or may not increase the corrosion susceptibility, depending not only on the metal-reinforcement combination but also on manufacturing process parameters. In this work, corrosion characteristics were examined and compared for three Al 7075-based MMCs prepared in the laboratory using the same procedure with carbon nanotubes (CNT).

2. Experimental

AA 7075 alloy has been taken as the matrix material. The chemical composition of the AA 7075 metal matrix is given in Table 1. Multi Wall Carbon Nanotubes- MWCNTs were synthesized by electric arc dis-charge method and purified by chemical method, used as the reinforcement [11]. The powders were mixed using Pestle and Mortar (manual method) for 1 h and the MWCNTs at different mass fraction (0.5, 1.0, 1.5, and 2.0) were added to the base alloy using shear mixer for 20 minutes. The blended powders were compacted using uniaxial press at 450 MPa to get a consolidated sample of 30 mm diameter. They were sintered and compacted. Then the samples were sliced and metallographically polished before the experiments were conducted.

Table 1. *Composition of AA 7075 (wt. %).*

Cr	Si	Mg	Cu	Zn	Al
0.1	0.4	2.5	1.6	5.5	Balance

2.1. Electrochemical Corrosion

The composites were machined and subjected to metal-lographic, and corrosion tests. The samples were polished with 1000 mesh SiC paper and degreased with acetone before testing. The corrosion resistance of bare and coated samples was evaluated in 3.5 wt. % NaCl solution. Samples of 1cm2 surface area were exposed to the solution. All elec-trochemical measurements were performed in a three elec-trode glass cell. Bare and coated specimens were used as working electrodes. The reference electrode was a saturated calomel electrode and the auxiliary electrode was platinum. The corrosion potential vs. current density was measured in 3.5 wt. % NaCl solution. The corrosion potential was rec-orded with respect to a saturated calomel electrode for a period of 1 h with time interval in seconds. The measure-ments of anodic polarization were made with regard to the corrosion potentials (E_{corr}).

3. Results and Discussion

XRD pattern of the MWNTs are shown in Figure 1. The peaks are indexed to the reflections of hexagonal graphite (peak (002) at 25.9˚, peak (101) at 43.3˚, peak (004) at 53.4˚ and a peak (110) at 78.4˚). The (002) peak arises due to interlayer stacking of graphene sheets.

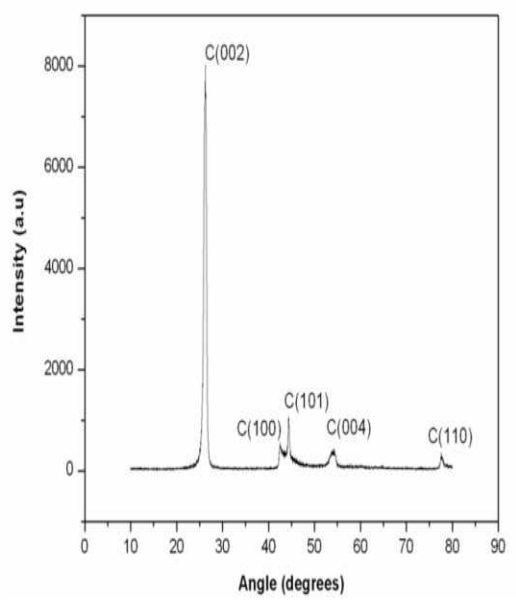

Figure 1. *XRD pattern of MWNT.*

The presence of this peak in the XRD spectra of CNTs indicates the concentric cylindrical nature of graphene sheets nested together and the nanotubes are multiwall in nature. The shift of the (002) reflection from 2θ = 26.4˚ for graphite 25.6˚ for the carbon nanotubes reveals an increase in the interlayer distance from 0.335 nm for graphite to 0.347 nm for the CNTs.

3.1. Raman Spectroscopy

Multi-walled carbon nanotubes (MWCNTs) prepared by the carbon arc method is composed of a coaxial arrangement of concentric nanotubes. The Raman spectra shown in Figure 2 provides experimental evidence for the coaxial structure. In many cases, however, MWCNTs have very large diameters compared with SWCNTs even for the innermost layer of the nanotube, and no one has yet succeeded in observing the RBMs in large diameter MWNTs. Hence in the present work, the RBM spectrum is not included in the report. The D-mode at 1350 cm^{-1} has been known in graphite for over a few decades and this is induced by disorder. In carbon nanotubes, this D-mode is observed at somewhat smaller frequency than in graphite and shifts at a rate between 38 and 65 cm^{-1}/eV with laser excitation [12]. The D-mode is usually lower than D-mode frequency of graphite and its intensity is quite large as compared to G-band. The bandwidth is 40 cm^{-1}. These two characteristics (frequency and line width) ensure that the sample is nanotube and not graphite [13].

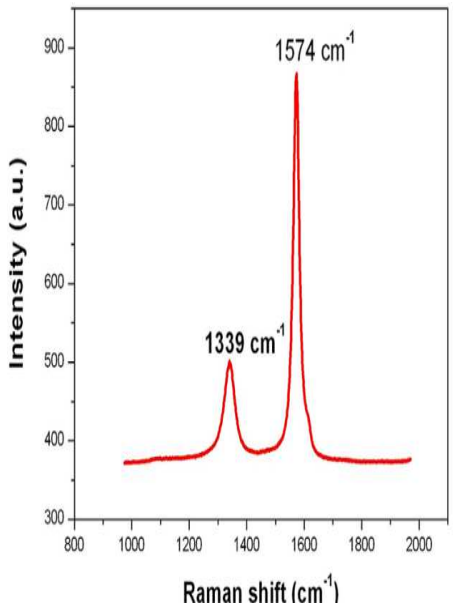

Figure 2. *Raman spectra of MWNTs.*

The observation of large D band peaks compared with the G peak intensity in MWCNTs bundles indicates the presence of amorphous carbon [13]. In graphite and carbon nanotubes, the G-band Raman vibrational mode is present due to in-plane vibrational movement of carbon atoms.

The observation of characteristic multi-peak features around 1580 cm^{-1} provides a signature of carbon nanotubes. Unlike graphite (tangential mode at 1582 cm^{-1}), the tangential G-mode in MWCNTs gives rise to a multipeak feature, also named the 61 G-band. These features have previously been reported [13-15], where the spectral profile resembles our spectra but with a difference in the peak positions. The

BWF line at 1540 cm^{-1} which is the characteristic of metallic type, is absent in the spectra. This, in turn, reinforces our suggestion that the grown nanotubes are of semiconducting type and not metallic. In MWCNT, there is a single peak at 1589 cm^{-1} corresponding again to the high-energy graphite like mode; the low energy RBM mode is generally not seen [15]. It confirms the nanotubes are in multi walled nature. Figure 3 shows the TEM image of Multi Wall Carbon Nanotubes.

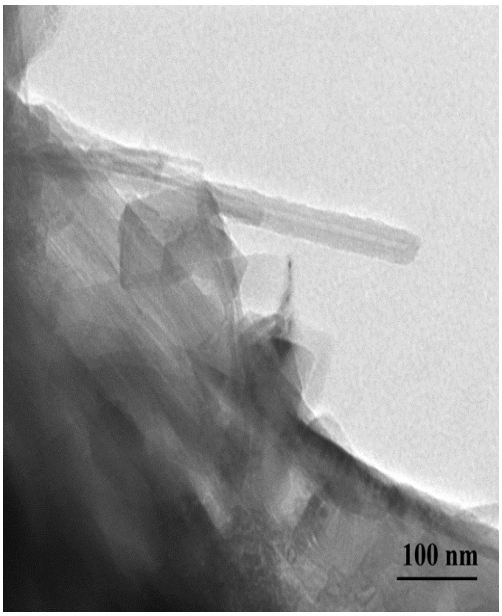

Figure 3. *TEM Image of MWNTs.*

X-Ray Diffraction study on Al7075/MWNTs composites is a major characterization technique to confirm the formation of phases in AA7075/MWNTs composites. Figure 4 shows the XRD pattern of AA7075 carbon nanotubes composites with increase wt% of MWNTs. The main purpose of XRD, here is to confirm the formation of Al4C3 phases. From Figure 4, it is clearly observed that the main phases formed is that of Zn and Al phases. Zn phase is a precipitate phase of Al-Zn-Mg alloys when at 450 OC.

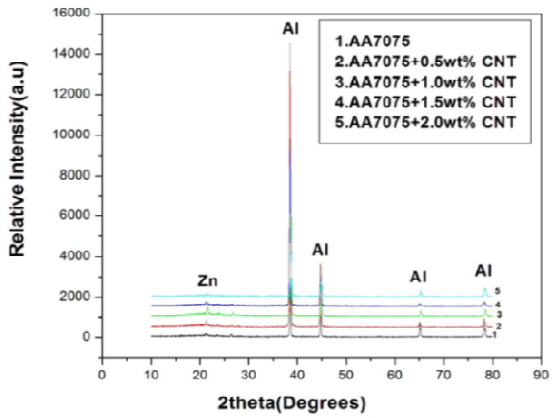

Figure 4. *XRD of AA7075+CNT nanocomposite with different compostion of CNTs.*

It should be noted that carbon peak is not seen for any of the 0.5 wt. %, 1.0 wt. %, 1.5 wt. % or 2.0 wt. % AA7075/MWCNTs composites, as can be due to that the content of carbon nanotubes with light ato-micity is too small to be examined by XRD. It is very in-teresting that the peak of Al_4C_3 phase also is not found suggesting that the reaction between carbon nanotubes and Al does not take place. Hence there is a possible increase of hardness and strength of the composites. Al_4C_3 is usually grown on the prismatic planes of carbon fiber and because the carbon atoms in the CNT shells behave like that they are in graphite basal plane. This restricts the formation Al4C3 nanocomposites. Therefore the peak observ in the synthesized composites show the absence of Al4C3.So here in synthesized composites the peak observations showed the absence of Al_4C_3.

The density of AA 7075 metal matrix composite and CNT reinforced Metal Matrix nano composite is given Table 2. The decrease in density may be due to formation of CNT agglomerates.

Table 2. Relative density of the reinforced nano composites.

AA7075 + x % CNT	**0 %**	**0.5%**	**1.0%**	**1.5%**	**2.0%**
Density(g/cm^3)	2.8657	2.7489	2.7852	2.8145	2.7773

3.1. Corrosion Studies

The polarization curves for AA 7075 and CNT reinforced AA 7075 composite (Figure 5) with various composition are examined in 3.5% NaCl. The E_{corr} , I_{corr} and the corrosion rate are estimated using Tafel polarization and Impedance techniques.

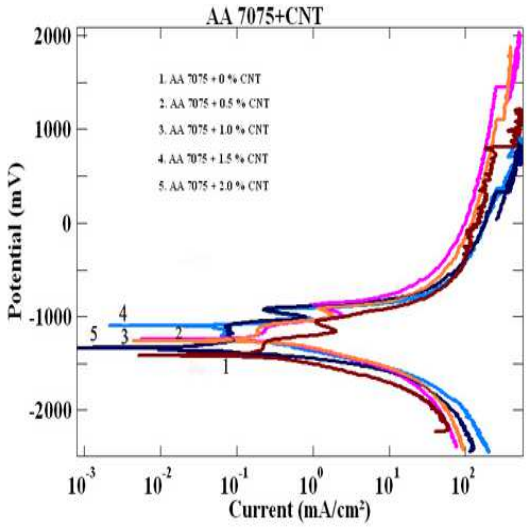

Figure 5. *Electrochemical polarization curve of CNT reinforced nanocomposite.*

The corrosion rate of the base material and different composition of CNT reinforced composite is given in the Table 3.

Table 3. *Corrosion Potential, Corrosion Current and Corrosion rate of the nanocomposite.*

AA7075+ x %CNT	I_{corr}(mA/cm$^{2)}$	Corrosion rate(mpy)
0% CNT	10.0887	4.2522056
0.5% CNT	22.6860	9.539528
1.0% CNT	35.5275	14.712354
1.5% CNT	47.6255	19.750038
2.0% CNT	48.1852	20.996654

In the equation, i_{corr} is substituted from the Tafel Extra-polated curve given by the instrument's software.

From the table it is observed that there is an increase in corrosion rate with respect to increase in wt% of CNT in the base alloy.

3.2. SEM Characterization

SEM mircrograph (Figure 6 a and b) shows the severity of the corrosion environment on 1.0 wt. % CNT reinforced AA7075 composite. The increase in the corrosion is due to the galvanic nature of the AA 7075 and CNT.

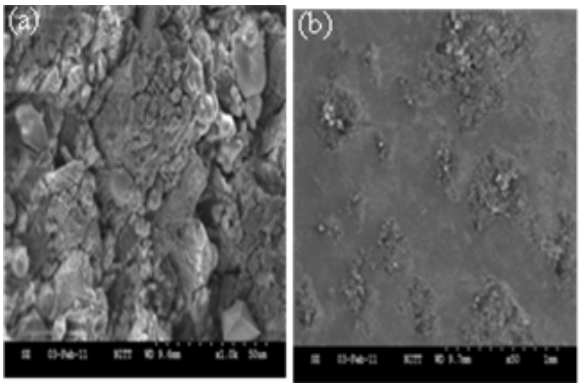

Figure 6*. SEM images of Corroded-CNT reinforced AA7075 nano composite sample at different magnification (1000x and 50x).*

3.3. Impedance Spectroscopy Study

Figure 7 shows the result obtained from the EIS measurements performed at the open circuit potential of the typical Nyquist plot with different composition of CNT–AA7075 composite immersed in 3.5 wt. % of NaCl solution solution as electrolyte solution.

It can be easily seen that the radius of the high frequency semicircle rapidly decreases from 2.0 % – 0.5%. The plot for base alloy with 0% CNT composite lies below all CNT reinforced composites. Higher frequency time-constant can be assigned to a capacitance of double layer on the surface of composite [16].

Low frequency constant is related to a diffusion limitation of the corrosion process. From impedance plots it may be seen that the activation control mechanism appears to be not operative. Also, no sign of film formation is noticed. The reactions predominantly undergo by diffusion control mechanism.

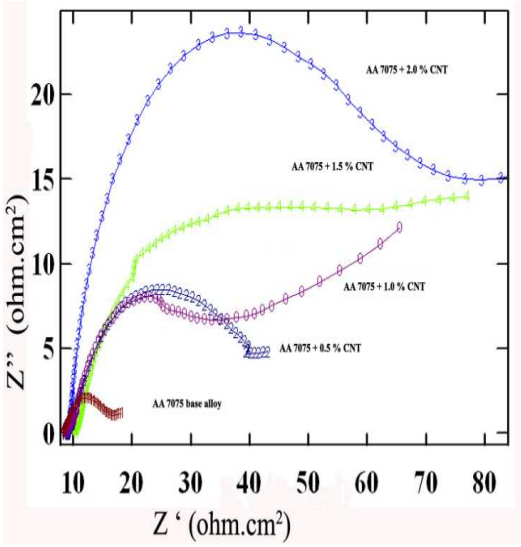

Figure 7. *Impedance plot of CNT reinforced nanocomposite.*

The reactions predominantly undergo by diffusion control mechanism. The results suggest that addition of CNT decreases corrosion resistance, which con-firms the result obtained by Tafel plot.

4. Conclusion

It has been generally observed that with increase in per-centage addition of CNT, the corrosion rate increases, which may be due to the anodic nature of the CNT in the matrix.

The reactions predominantly undergo by diffusion con-trol mechanism.

Acknowledgements

Technical assistance and help received from Mr. Jaganathan. M, Department of Metallurgy, IITM, Chennai & Dr. M.S Senthil Saravanan, NIT, Trichy is acknowledged.

Our sincere thanks due to the authorities of MME department, NIT-T, for rendering necessary facility utilized for this investigation.

References

[1] Ijima, "Helical microtubules of graphitic carbon," Nature, , pp.354–56, 1991.

[2] D.M. Aylor and P.J. Moran, J. Eletrochem. Soc., 132 , pp.1277, 1985.

[3] P.P. Trzaskoma, E. McCafferty and C.R. Crowe, J. Eleetro-chem. Soc., vol. 130, 1804, 1983.

[4] K. Noda, H. Ono, H. Tsuru, H. Tezuka and A. Kamio, J. Jpn. Inst. Met., vol. 56, 641,1992.

[5] H. Sun, E.Y. Koo and H.G. Wheat, Corrosion, 47, 741, 1991.

[6] M.M. Buarzaigaand S.J. Thorpe, Corrosion, 50, 176, 1994.

[7] P.P. Trzaskoma, Corrosion, 46, 402, 1990.

[8] W.F. Czyrklis, presented at CORROSION/85, paper No.196, 1985.

[9] D.M. Aylor and R.M. Kain, ASTM STP, vol. 864,pp.632, 1983.

[10] L.H. Hihara and R.M. Latanision, Corrosion, vol. 48, 546, 1992.

[11] M.S.SenthilSaravanan, S.P.KumareshBabu, K.Sivaprasad and S.Jagannatham, Intl.J.Engg.Sci.Ttech., vol. 2, pp.100, 2010.

[12] J.Kastner et al., "Resonance Raman and infrared spectroscopy of carbon nanotubes," Chem. Phys. Let., vol. 221, pp. 53–58, 1994.

[13] A.M. Rao et al., "Diameter-selective Raman scattering from vibrational modes in carbon nanotubes," Science, vol. 275, pp. 187–190, 1997.

[14] A. Jorio, "Polarized Raman Study of Single-Wall Semi-con-ducting Carbon Nanotubes," Phys. Rev. Lett., vol. 85, pp. 2617, 2000.

[15] Thomsen, C., "Second-order raman spectra of single and multi-walled carbon nanotubes," Phys. Rev. B, vol. 61, pp. 4542–4544, 2000.

[16] Weifeng Xu, Jinhe Liu, "Microstructure and pitting corrosion of Friction stir welded joints in 2219-O Alumiunum alloy thick plate," Corrosion Science, Elsevier, vol.51, pp. 2743–275, 2009.